Integrative Transcriptomic Analysis Reveals Synaptic Pathway-Enriched Prognostic Gene Signature in Glioblastoma

Vivin Andriani, S.Si., M.Sc.[1], Fenny Fitriani, S.Si., M.Si.[2], Sari Setyo Ningrum[2], Gangga Anuraga, Ph.D.[2,*]

[1]Department of Biology, Faculty of Engineering and Science, Universitas PGRI Adi Buana Surabaya, Indonesia, [2]Department of Statistics, Faculty of Engineering and Science, Universitas PGRI Adi Buana Surabaya, Indonesia.

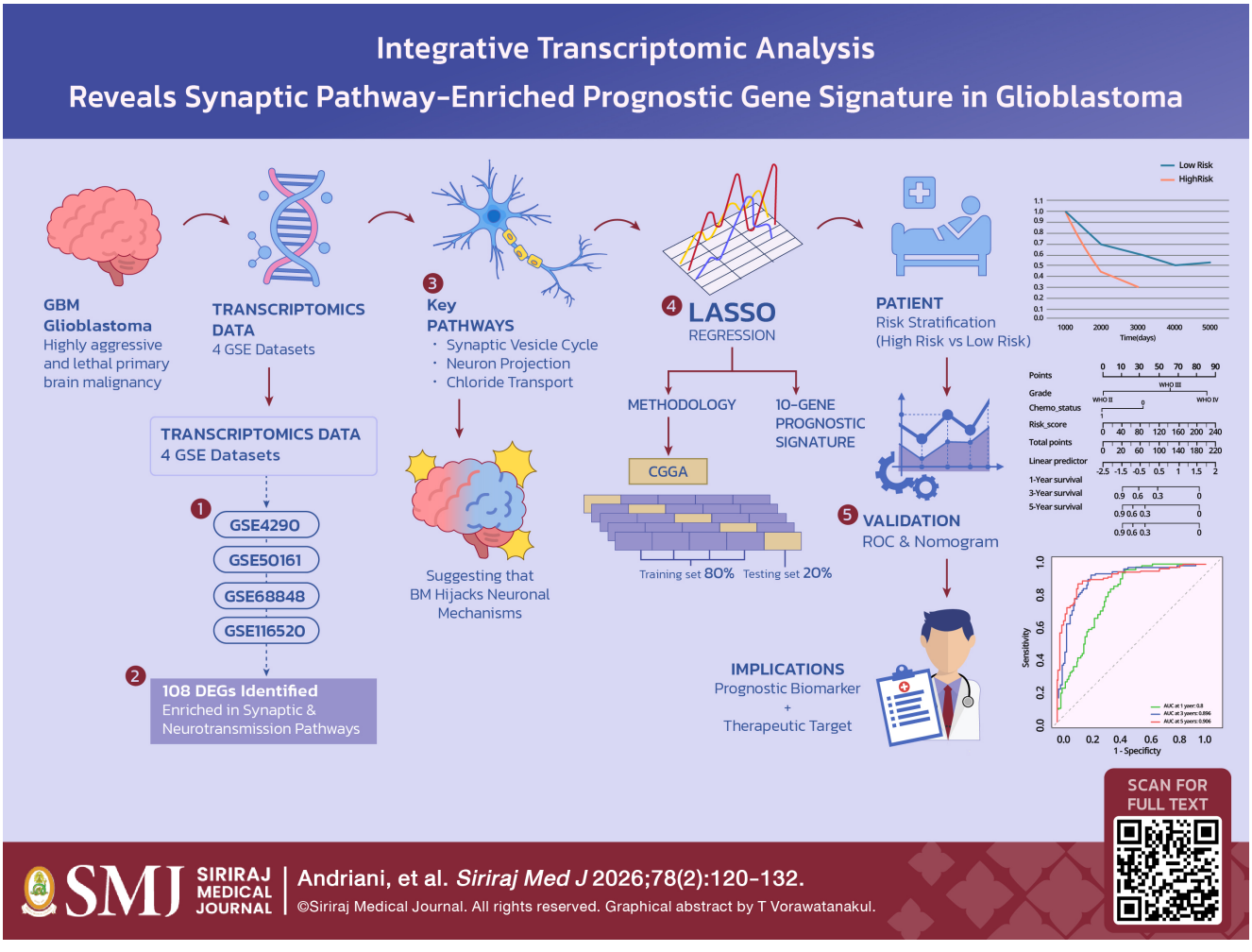

*Corresponding author: Gangga Anuraga
E-mail: g.anuraga@unipasby.ac.id
Received 29 September 2025 Revised 29 November 2025 Accepted 22 December 2025
ORCID ID:http://orcid.org/0000-0002-0902-3968
https://doi.org/10.33192/smj.v78i2.277969

ABSTRACT

Objective: This study aimed to elucidate the transcriptomic landscape of glioblastoma (GBM) by integrating multiple datasets to identify prognostically significant gene signatures and investigate the involvement of synaptic pathways.

Materials and Methods: Four transcriptomic datasets were analyzed using the limma pipeline for differential gene expression analysis with empirical Bayes moderation to identify differentially expressed genes (DEGs). Functional enrichment analyses were conducted via Gene Ontology and KEGG. A prognostic model was constructed using LASSO-Cox regression on the CGGA mRNAseq_693 cohort (n=693) and validated on the CGGA_325 cohort (n=325). Multivariate Cox proportional hazards regression assessed the model's independent prognostic value. External validation of gene expression was performed using TCGA (n=163) and GTEx (n=207) datasets.

Results: A total of 108 consistently dysregulated DEGs were identified, enriched in synaptic vesicle cycling, neuronal projection, and chloride transport pathways. A robust ten-gene prognostic signature (SPRY1, CD58, RCC1, E2F7, BUB1, FAM46A, TYMS, NEDD9, CHST14, REPS2) effectively stratified patients, with time-dependent ROC AUCs of 0.718, 0.755, and 0.757 at 1-, 3-, and 5-year survival points. Multivariate Cox analysis confirmed the model's independent prognostic value, further refined by a nomogram with AUCs of 0.8, 0.898, and 0.906. Differential expression of all ten genes was validated externally.

Conclusion: This study reveals a previously underexplored synaptic pathway-related gene signature with strong prognostic relevance for GBM. The ten-gene model offers a clinically applicable tool for risk stratification and highlights neuron-tumor synaptic interactions as critical drivers of tumor progression, providing a foundation for future therapeutic strategies.

Keywords: Glioblastoma; transcriptomics; prognostic model; synaptic pathways; differentially expressed genes (Siriraj Med J 2026;78(2):120-132)

INTRODUCTION

Glioblastoma (GBM) is the most aggressive and lethal primary brain tumor, characterized by rapid progression and poor patient survival despite advances in surgical, radiotherapeutic, and chemotherapeutic interventions.[1] The median survival time remains approximately 15 months, underscoring the urgent need for improved prognostic biomarkers and therapeutic strategies for this disease.[1,2] Recent research has increasingly recognized the critical role of synaptic signaling in the pathophysiology of GBM.[3-5] Neuron-glioma synaptic interactions have been shown to facilitate tumor growth, invasion, and resistance to treatment by creating a tumor-supportive microenvironment.[6-8] These findings position synaptic pathways as promising targets for both prognostic biomarker discovery and novel therapeutic interventions.

Transcriptomic profiling serves as a systematic approach to explore biological processes by linking synaptic-associated gene expression with clinical outcomes,[9-12] thereby offering a precise strategy for developing prognostic models with biological relevance. This methodology facilitates the identification of differentially expressed genes (DEGs) that can act as prognostic markers or therapeutic targets. However, despite numerous transcriptomic studies, the integration of multiple datasets to construct robust, biologically informed prognostic models remains a challenge. Focusing specifically on synaptic pathway-related genes offers a targeted strategy to uncover the functional impact of neuron-tumor synaptic interactions on GBM progression.

This study employed integrative bioinformatics analyses of multiple publicly available GBM transcriptomic datasets to identify DEGs enriched in synaptic processes and correlated with patient prognosis. Through rigorous statistical modeling, including LASSO-Cox regression and multivariate Cox proportional hazards analyses, a synaptic pathway-enriched gene signature with strong prognostic value was constructed and validated in the TCGA cohort. This signature not only effectively stratifies patients but also highlights the molecular mechanisms underlying tumor progression mediated by synaptic signaling.

By bridging transcriptomic insights with the biological mechanisms of neuron-glioma interplay, this study advances the understanding of the GBM's molecular drivers of GBM. The identified gene signature enhances risk stratification beyond current prognostic markers, offering a clinically applicable tool for personalized management of patients. Furthermore, it provides a foundation for the development of targeted therapies aimed at disrupting tumor-promoting synaptic communication, which could improve treatment outcomes.

In summary, this synaptic-centric transcriptomic investigation addresses a critical gap in GBM research by integrating pathway-specific molecular data with clinical prognostic data. These findings provide novel insights into the role of synaptic signaling in GBM progression and present a validated prognostic model with potential clinical utility. This study supports the ongoing pursuit of precision medicine approaches that incorporate tumor microenvironmental interactions to improve prognosis and therapeutic efficacy in this devastating disease.

MATERIALS AND METHODS

Gene expression data acquisition and preprocessing

The gene expression data utilized in this study were derived from multiple publicly available microarray datasets. Four datasets—GSE4290,[13] GSE50161,[14] GSE68848,[15] and GSE11652016—were retrieved from the Gene Expression Omnibus (GEO) database (http://www.ncbi.nlm.nih.gov/geo/). These four GEO datasets were selected based on predefined criteria, including availability of both GBM and normal tissues, sufficient sample size, comparable profiling platforms, and high-quality normalized expression data enabling integrative analysis. Specifically, GSE4290, GSE50161, and GSE68848 were based on the Affymetrix Human Genome U133 Plus 2.0 Array (GPL570 platform), encompassing a total of 339 glioblastoma (GBM) tumor samples and 64 normal brain tissue samples. The GSE116520 dataset, generated using the Illumina HumanHT-12 V4.0 platform (GPL10558), comprises 17 GBM tumor samples and 8 normal controls, offering a comprehensive transcriptomic landscape for identifying robust DEGs.

Prognostic modeling employed gene expression and survival data from the mRNAseq_693 cohort of the CGGA (https://www.cgga.org.cn/index.jsp), constructing a LASSO-Cox risk model,[17,18] with clinical validation and nomogram development conducted using the CGGA_325 cohort. Expression validation of prognostic candidates was further corroborated using TCGA and GTEx datasets, enabling comparative analysis between GBM and normal brain tissues.

Identification of DEGs

DEGs were conducted using the "limma" package in R (v4.3.0), identifying DEGs based on $|\log2FC| > 1$ and $p < 0.05$, with Benjamini-Hochberg correction for false discovery rate. Venn diagram analysis (https://bioinfogp.cnb.csic.es/tools/venny/index.html) was employed to identify overlapping DEGs across datasets, with subsequent functional enrichment analysis to elucidate their biological relevance in GBM pathophysiology.

Functional enrichment analysis to elucidate biological relevance

Functional enrichment analysis was performed using the Enrichr platform (https://maayanlab.cloud/Enrichr/),[19-21] encompassing gene ontology (GO) analysis to elucidate overrepresented biological processes (BP), cellular components (CC), and molecular functions (MF),[22] alongside KEGG pathway analysis to delineate the involvement of DEGs in key signaling and metabolic pathways.[23] Input gene lists comprising DEGs with FDR-adjusted p-values below 0.05 were analyzed via Enrichr, prioritizing top-enriched GO terms and KEGG pathways based on a combined score that integrates p-value and z-score, thereby revealing key molecular mechanisms underlying GBM pathophysiology.

Construction of prognostic risk model via LASSO-Cox regression

The CGGA mRNAseq_693 dataset was randomly partitioned into training (80%) and testing (20%) subsets using stratified sampling based on survival status, with reproducibility ensured by applying a fixed random seed (set.seed = 123). LASSO regression was employed for simultaneous feature selection and model regularization,[17,24,25] with five-fold cross-validation to determine the optimal λ, minimizing prediction error and enhancing model generalizability.

The LASSO model was validated using the independent testing set, with risk scores calculated as a linear combination of gene expression values weighted by the LASSO-derived coefficients. Correlation analysis was conducted to assess gene-risk score associations, with the top ten genes visualized in a bar plot to delineate risk-promoting versus protective genes based on the direction and magnitude of their impact.

To evaluate the clinical utility of the risk score, patients in the test cohort were stratified into high- and low-risk groups based on the median risk score, followed by Kaplan–Meier survival analysis to compare overall survival.[18,26,27] Time-dependent ROC curves at 1, 3, and 5 years were generated to assess model discriminative power, with AUC values calculated to quantify predictive accuracy.

Clinicopathologic correlation analysis

Patients were stratified into high- and low-risk groups based on the median risk score. Differences in clinical characteristics were assessed using the Wilcoxon rank-sum test for Age (continuous variable) and Chi-square tests for categorical variables, including Gender, WHO Grade, Radiotherapy status, Chemotherapy status,

MGMT methylation status, and IDH mutation status. Statistical significance was defined as $p < 0.05$.

Independent prognostic factor analysis and nomogram construction

Cases with missing values in essential clinical variables, such as survival data, MGMT methylation, or IDH mutation status, were excluded from the multivariate Cox analysis, and no imputation was performed. The multivariate Cox regression analysis was conducted within the CGGA_325 cohort to assess the independent prognostic significance of the gene expression-derived risk score in conjunction with clinical and molecular variables, including age, gender, tumor grade, treatment status, MGMT methylation, and IDH mutation status, with hazard ratios (HRs) calculated at $p < 0.05$.

A prognostic nomogram was constructed using statistically significant variables,[28] assigning scores based on regression coefficients to predict 1-, 3-, and 5-year survival probabilities, with predictive accuracy assessed via time-dependent ROC curves and AUC values.[26,27] The CGGA_325 cohort showed comparable demographic characteristics to the CGGA mRNAseq_693 training cohort, particularly in terms of age distribution and sex proportion, supporting its suitability for external validation.

Expression validation of LASSO-selected genes utilizing GEPIA

Boxplot analyses performed via GEPIA, utilizing log2 (TPM + 1) normalization, $|\log2 \text{ fold change}| \geq 1$, and $p < 0.01$,[29] demonstrated significant differential expression of all selected genes between tumor and normal tissues, with most exhibiting marked overexpression in GBM samples, reinforcing their oncogenic potential and validation for inclusion in the LASSO-based prognostic model.

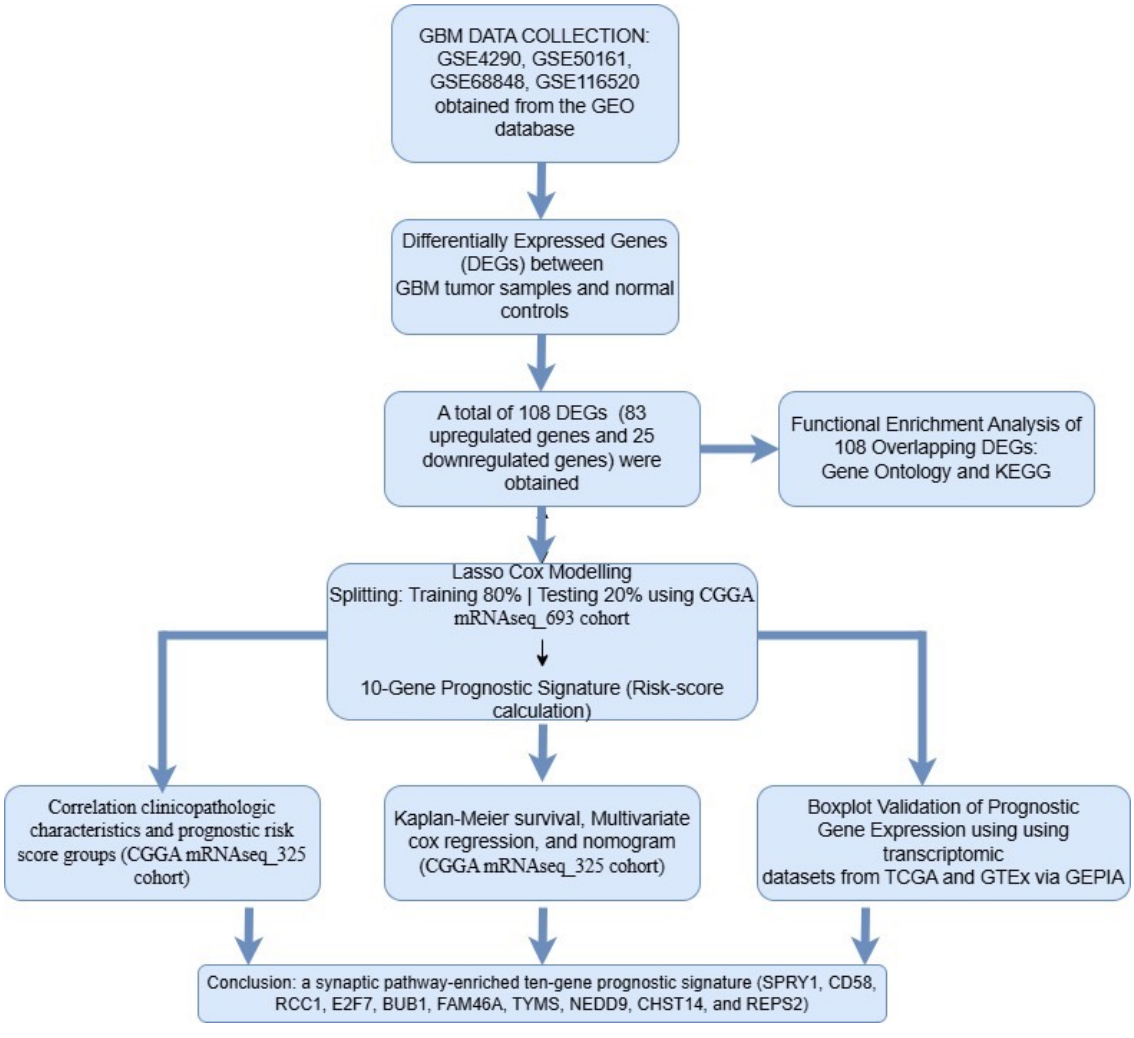

Fig 1. Overview of the study workflow. Transcriptomic datasets (GSE4290, GSE50161, GSE68848, GSE116520) were integrated for the screening of differentially expressed genes (DEGs), followed by synaptic-pathway enrichment and LASSO Cox modeling to develop a 10-gene prognostic signature. Validation was conducted using survival curves, receiver operating characteristic (ROC) analysis, and nomogram assessment. Clinical correlation analysis associated risk scores with grade, IDH status, and age, underscoring its potential clinical applicability.

RESULTS

Identification of DEGs and enrichment analysis in GBM

A comprehensive analysis was conducted involving 356 GBM tissue samples and 72 normal tissue samples. Each dataset was individually processed and analyzed using R software to generate lists of DEGs. Specifically, the GSE4290, GSE50161, GSE68848, and GSE116520 datasets were systematically examined, yielding 4,631 DEGs (2,284 upregulated, 2,349 downregulated), 5,385 DEGs (2,523 upregulated, 2,862 downregulated), 6,493 DEGs (3,412 upregulated, 3,081 downregulated), and 3,370 DEGs (1,862 upregulated, 1,508 downregulated), respectively (Fig 2A–D). Integration of datasets using a Venn diagram analysis identified 83 consistently upregulated DEGs (log2FC > 1) and 25 consistently downregulated DEGs (log2FC < -1) across all four datasets (Fig 2E, F).

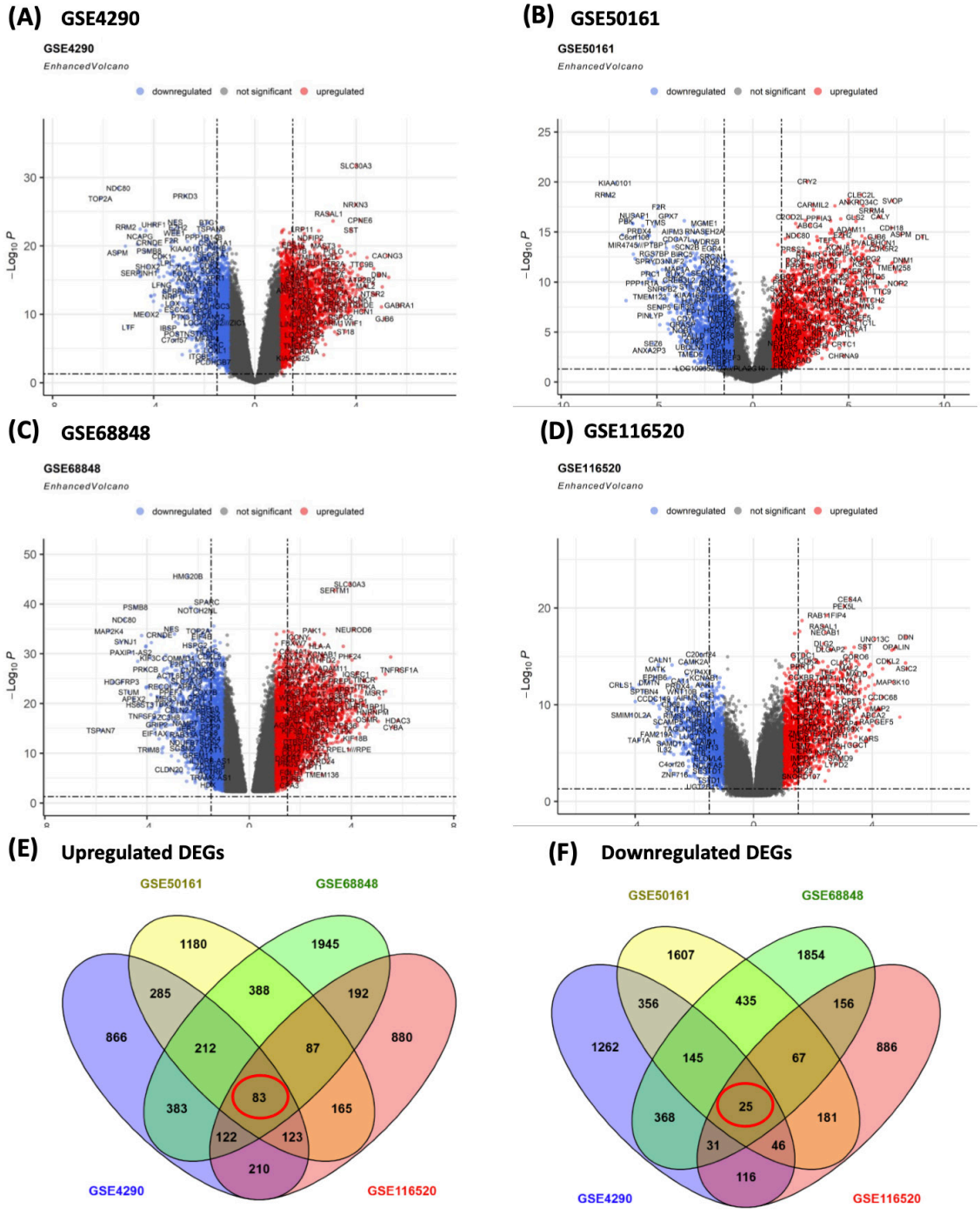

Fig 2. Identification of Differentially Expressed Genes (DEGs) in GBM Across Multiple Datasets. (A–D) Volcano plots illustrating DEGs across four GBM datasets, highlighting upregulated genes (log2FC ≥ 1, p < 0.05) in red, downregulated genes (log2FC ≤ -1, p < 0.05) in blue, and non-significant genes in gray, with log2 fold change on the x-axis and -log10(p) values on the y-axis. **(E, F)** Venn diagrams depicting the intersection of DEGs across GSE50161, GSE68848, GSE4290, and GSE116520, identifying 83 consistently upregulated **(E)** and 25 consistently downregulated DEGs **(F)**, potentially representing pivotal molecular drivers and candidate biomarkers in GBM pathogenesis.

GO and KEGG pathway enrichment analyses of the 108 overlapping DEGs in GBM revealed significant associations with neuronal projection, synaptic function, and chloride transmembrane transporter activity (Fig 3A–D). As shown in Fig 3A, the most significantly enriched BPs included chemical synaptic transmission (GO:0050804), positive regulation of catecholamine secretion (GO:0033605), and the synaptic vesicle cycle (GO:0099504). The synaptic vesicle cycle, a neuronal mechanism traditionally implicated in neurotransmitter release and recycling[30] has been increasingly recognized for its role in the synaptic integration of high-grade gliomas within neural networks, a process that significantly contributes to glioma progression in both preclinical models[4,31] and clinical patient samples.[32]

Cellular component (CC) analysis further identified significant enrichment in neuron projection (GO:0043005), exocytic vesicle membrane (GO:0099501), and synaptic vesicle membrane (GO:0030672) (Fig 3B). Meanwhile, molecular function (MF) analysis highlighted the enrichment of guanyl-nucleotide exchange factor activity (GO:0005085), protein heterodimerization (GO:0046982), and chloride transmembrane transporter activity (GO:0015108) (Fig 3C).

KEGG pathway analysis revealed significant enrichment in pathways associated with the synaptic vesicle cycle, neuroactive ligand-receptor interaction, insulin secretion, and GABAergic synapse (Fig 3D), highlighting the potential involvement of synaptic and neurotransmission-related genes in GBM pathogenesis and identifying promising therapeutic targets to disrupt tumor-neuron crosstalk.

LASSO analysis for prognostic gene identification in GBM

LASSO-Cox regression was applied to the 108 GBM-associated genes to construct a prognostic model, with the coefficients of selected genes plotted against the lambda parameter, illustrating the reduction of non-zero coefficients and refinement of a parsimonious model (Fig 4A). The optimal lambda value, balancing model complexity and predictive accuracy, was determined by plotting partial likelihood deviation against log(λ) (Fig 4B).

The analysis identified ten pivotal prognostic markers—SPRY1, CD58, RCC1, E2F7, BUB1, FAM46A, TYMS, NEDD9, CHST14, and REPS2—as the most robust predictors (Fig 4C), with correlation heatmap

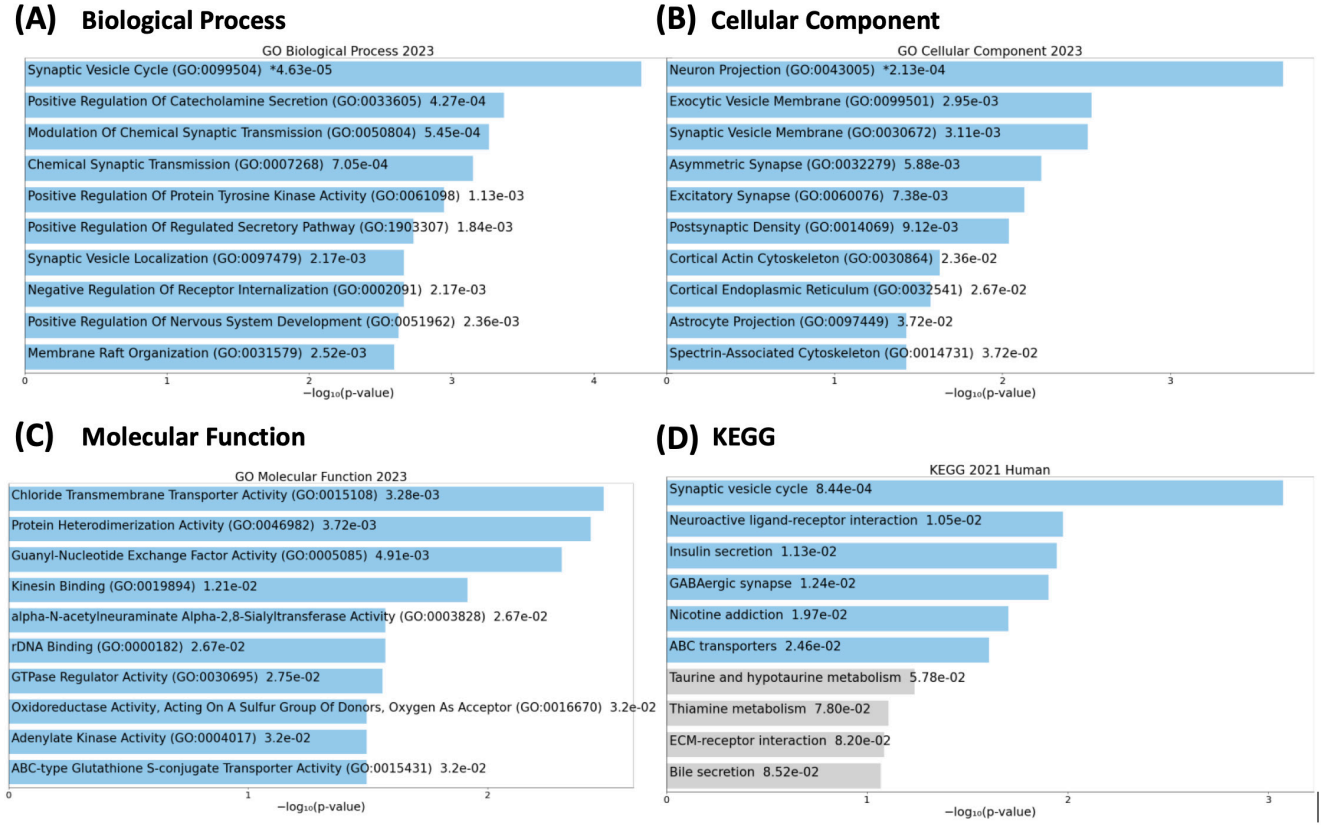

Fig 3. Functional Enrichment Analysis of 108 Overlapping DEGs in Glioblastoma (GBM). Bar plots illustrate significantly enriched GO terms across **(A)** Biological Processes, **(B)** Cellular Components, and **(C)** Molecular Functions, with **(D)** KEGG Pathway Analysis emphasizing pathways implicated in synaptic function, neurotransmission, and tumor-neuron interactions.

analysis revealing significant co-expression patterns (Fig 4D). The ten-gene signature effectively stratified patients into high- and low-risk groups, with Kaplan-Meier analysis indicating markedly worse survival in the high-risk group (Fig 4E). Time-dependent ROC analysis demonstrated progressive enhancement in predictive accuracy, with AUC values of 0.718, 0.755, and 0.757 for 1-, 3-, and 5-year overall survival, respectively (Fig 4F), underscoring the prognostic relevance of the gene signature in GBM.

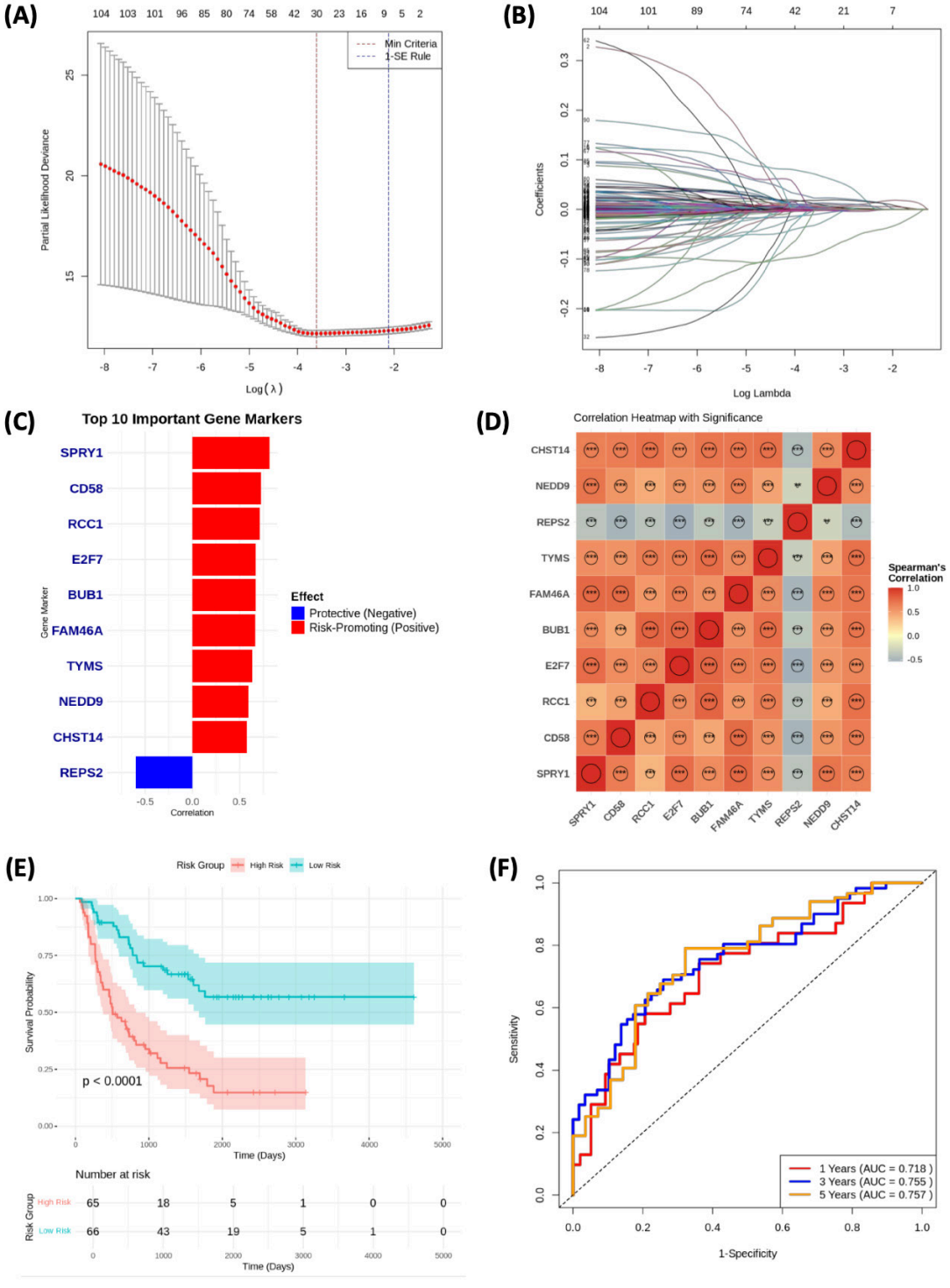

Fig 4. LASSO Analysis of Prognostic Genes Derived from DEGs in GBM. (A) Gene coefficients plotted against the lambda (λ) parameter, illustrating the reduction in non-zero coefficients as λ increases. **(B)** Partial likelihood deviation vs. log(λ), with the optimal λ value marked, balancing model complexity and predictive accuracy. **(C)** Ten most prognostic marker genes identified by LASSO as key predictors in GBM. **(D)** Correlation heatmap depicting the co-expression patterns of the top ten genes, with color intensity reflecting correlation strength (red: positive, blue: negative). **(E)** Kaplan-Meier survival analysis stratifying patients into high- and low-risk groups, revealing significantly worse survival in the high-risk cohort (log-rank $p < 0.05$). **(F)** Time-dependent ROC curves demonstrating the prognostic model's predictive accuracy over 1-, 3-, and 5-year intervals, with AUC values of 0.718, 0.755, and 0.757, respectively.

Correlation analysis of clinical variables and risk score stratification

To explore the clinical relevance of the prognostic model, we examined associations between the risk score and patient clinicopathologic variables. As summarized in Table 1, patients in the High-risk group exhibited a significantly greater proportion of WHO grade IV tumors and a higher frequency of IDH–wild-type status (both $p < 0.05$), indicating increased malignancy in this group. Chemotherapy-treated cases were more common in the High-risk group, whereas no significant differences were observed for gender or MGMT methylation status (all $p > 0.05$). Age was significantly higher in the High-risk group based on the Wilcoxon comparison, suggesting that older individuals tend to fall into higher-risk molecular subgroups.

Independent prognostic factors for GBM

Multivariate Cox regression analysis evaluated the independent prognostic value of the risk score alongside clinical variables, with tumor grade (WHO III: $p = 2.50 \times 10^{-6}$; WHO IV: $p = 6.54 \times 10^{-13}$), chemotherapy status ($p = 0.0028$), and risk score ($p = 2.54 \times 10^{-5}$) emerging as significant predictors of overall survival in GBM patients (Fig 5A).

A prognostic nomogram was subsequently developed by integrating the risk score with clinical parameters, assigning weighted point values to estimate 1-, 3-, and 5-year survival probabilities (Fig 5B). Time-dependent ROC analysis demonstrated the model's robust predictive performance, with AUC values of 0.8, 0.898, and 0.906 for 1-, 3-, and 5-year survival, respectively, underscoring its prognostic utility in GBM (Fig 5C).

Validation of prognostic gene expression in GBM

The expression profiles of ten prognostic genes identified through LASSO regression—SPRY1, CD58, RCC1, E2F7, BUB1, FAM46A, TYMS, NEDD9, CHST14, and REPS2—were validated using transcriptomic datasets from TCGA and GTEx, comparing GBM tumor tissues (n = 163) and normal brain tissues (n = 207). All ten genes demonstrated statistically significant differential

TABLE 1. Association between clinicopathologic characteristics and prognostic risk score groups.

Variable	Category	Low risk	High risk	P value	Sig
Age (years, median [IQR])		39 [IQR 11]	45 [IQR 17]	< 0.001	***
Gender	Female	70 (42.9%)	52 (32.1%)	0.0569	n.s.
	Male	93 (57.1%)	110 (67.9%)	0.0569	n.s.
Grade	WHO II	94 (57.7%)	9 (5.7%)	0.0000	***
	WHO III	38 (23.3%)	41 (25.9%)	0.0000	***
	WHO IV	31 (19%)	108 (68.4%)	0.0000	***
Radiotherapy status	Untreated	130 (82.3%)	114 (75%)	0.1538	n.s.
	Treated	28 (17.7%)	38 (25%)	0.1538	n.s.
Chemotherapy status	Untreated	85 (55.9%)	108 (71.1%)	0.0088	**
	TMZ Treated	67 (44.1%)	44 (28.9%)	0.0088	**
MGMT methylation status	methylated	82 (54.7%)	75 (48.1%)	0.2990	n.s.
	unmethylated	68 (45.3%)	81 (51.9%)	0.2990	n.s.
IDH mutation status	Mutant	128 (79%)	47 (29%)	0.0000	***
	Wildtype	34 (21%)	115 (71%)	0.0000	***

Significance indicators: *p < 0.05, **p < 0.01, ***p < 0.001
Abbreviation: n.s. = not significant

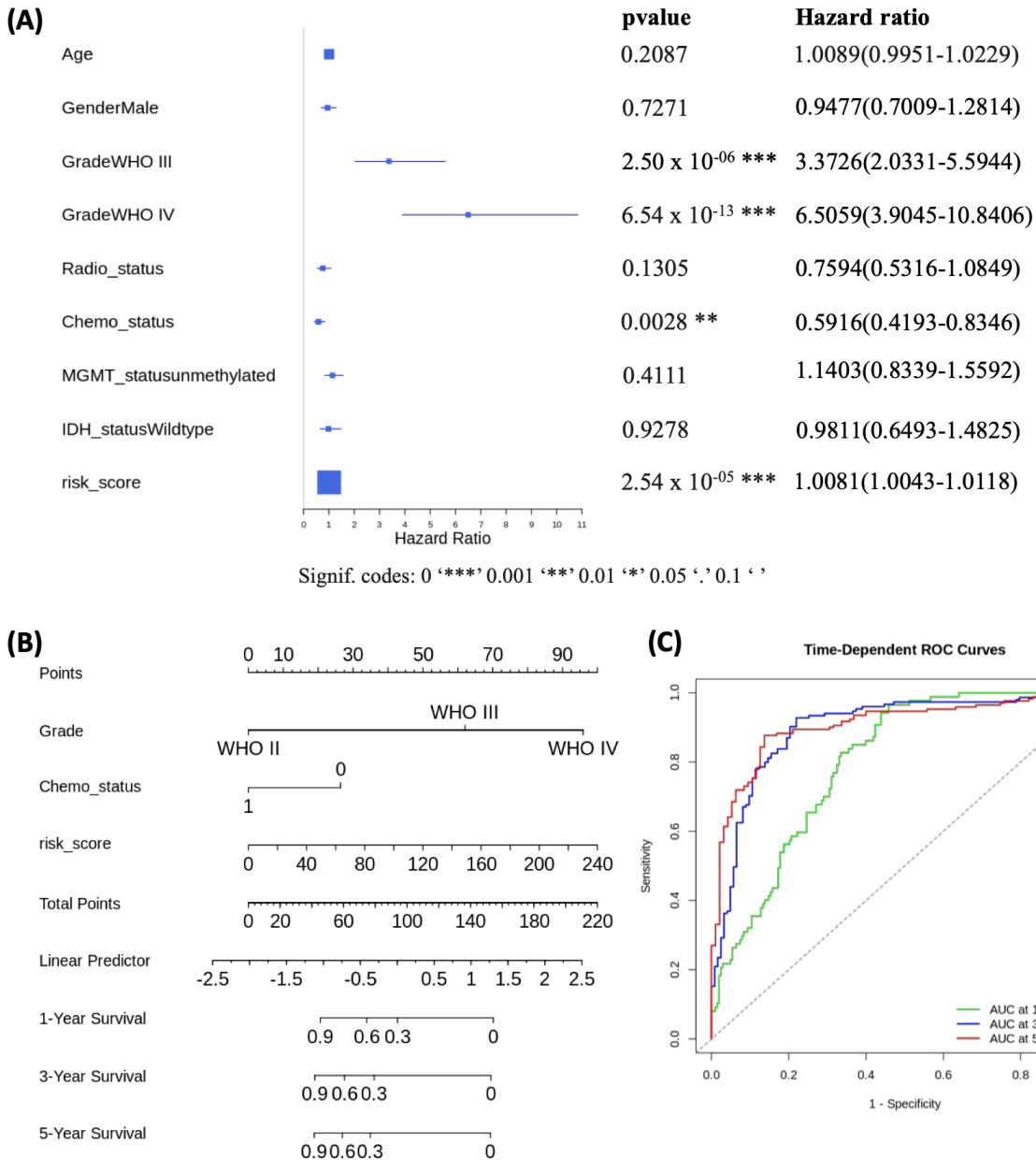

Fig 5. Independent Prognostic Factors in GBM. (A) Forest plot from multivariate Cox regression analysis assessing the prognostic independence of the risk score relative to clinical parameters, including age, gender, WHO grade, radiotherapy, chemotherapy, MGMT methylation, and IDH mutation, with HRs and 95% CIs indicated (**p < 0.01, ***p < 0.001). **(B)** Prognostic nomogram integrating the risk score and key clinical variables to estimate 1-, 3-, and 5-year survival probabilities in GBM, with points assigned to each parameter and summed to derive the total risk score. **(C)** Time-dependent ROC curves illustrating the predictive accuracy of the nomogram for 1-year (green), 3-year (blue), and 5-year (red) survival, with AUC values of 0.8, 0.898, and 0.906, respectively, underscoring robust temporal predictive performance.

expression ($p < 0.05$), with SPRY1, CD58, RCC1, E2F7, BUB1, FAM46A, TYMS, NEDD9, and CHST14 exhibiting marked upregulation, indicating potential oncogenic roles, while REPS2 showed significant downregulation, suggesting a tumor suppressor function (Fig 6). These findings reinforce the prognostic relevance of the selected genes, underscoring their potential as biomarkers for GBM pathogenesis and clinical stratification.

DISCUSSION

This study utilized a comprehensive bioinformatics framework to identify key differentially expressed genes (DEGs) and establish a prognostic model in glioblastoma multiforme (GBM), contributing novel insights into tumor biology and revealing potential biomarkers and therapeutic targets. Integration of four GEO datasets (GSE4290, GSE50161, GSE68848, and GSE116520)

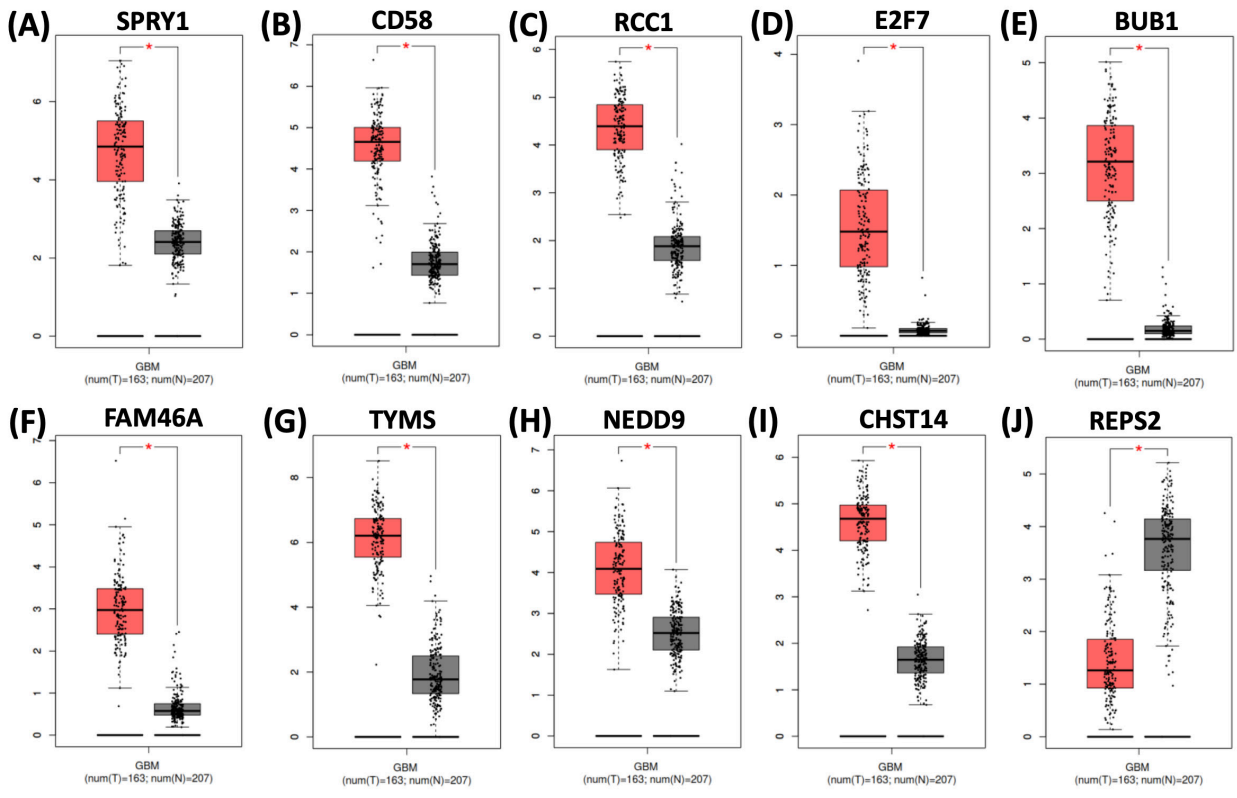

Fig 6. Differential Expression Analysis of LASSO-Identified Prognostic Genes in GBM. (A-J) Box plots illustrate the mRNA expression levels of ten LASSO-selected prognostic genes— SPRY1, CD58, RCC1, E2F7, BUB1, FAM46A, TYMS, NEDD9, CHST14, and REPS2—in GBM tumor tissues (n = 163) versus normal brain tissues (n = 207) using TCGA and GTEx datasets. Red box plots denote GBM samples, while grey box plots represent normal tissues, with asterisks (*) indicating statistically significant differential expression ($p < 0.05$). Group expression differences were evaluated using Student's t-test. Most genes, except REPS2, exhibited marked upregulation in GBM, underscoring their oncogenic potential, whereas REPS2 was significantly downregulated, suggesting a tumor suppressor role. These expression profiles further validate the diagnostic and prognostic relevance of the gene signature in GBM.

identified 108 overlapping DEGs—83 upregulated and 25 downregulated—predominantly enriched in synaptic-associated biological processes and signaling pathways. Notably, the enrichment of neuron projection, synaptic vesicle cycling, and chloride transmembrane transport pathways suggests that GBM cells may functionally integrate into neuronal networks. This observation is consistent with emerging evidence indicating that glioma cells exploit synaptic mechanisms to enhance proliferation, invasion, and therapeutic resistance, underscoring neuron–glioma interactions as pivotal determinants of GBM progression.[33-36] These synaptic-like mechanisms, including GABAergic neurotransmission, represent an underexplored but promising therapeutic axis requiring further mechanistic and pharmacologic investigation.[37-40]

Using LASSO regression, we identified a ten-gene prognostic signature (SPRY1, CD58, RCC1, E2F7, BUB1, FAM46A, TYMS, NEDD9, CHST14, REPS2) with diverse regulatory roles across cancer types. Several components of this signature—such as SPRY1 in MAPK signaling,[41] CD58-mediated immune modulation,[42] RCC1 in mitotic regulation,[43-45] and E2F7 in cell-cycle control[46-48] —have been implicated in oncogenic progression. Likewise, BUB1 family kinases contribute to chromosomal instability,[49-51] and upregulation of FAM46A,[52] TYMS,[53-55] NEDD9,[56-58] and CHST14[59] has been associated with aggressive tumor phenotypes, while REPS2 exhibits tumor-suppressive properties in several malignancies.[60] Collectively, these genes encompass biological pathways central to cell-cycle progression, apoptosis, immune evasion, and metastasis.

The ten-gene model demonstrated strong prognostic capacity, with AUC values of 0.718, 0.755, and 0.757 for 1-, 3-, and 5-year overall survival, respectively, comparable to or surpassing previously published signatures.[61,62] Importantly, multivariate Cox analysis confirmed the risk score as an independent prognostic factor alongside clinical variables such as tumor grade and chemotherapy status, and integration into a nomogram further improved predictive performance, achieving an AUC of 0.906 at 5 years.[63,64] Expression validation in TCGA and GTEx datasets corroborated the differential expression patterns of all ten genes, including downregulation of REPS2, consistent with its tumor-suppressive role.[65]

Our clinicopathologic correlation analysis further

supported the biological and clinical relevance of the risk model. High-risk patients were more frequently diagnosed with WHO grade IV tumors and IDH wild-type status, consistent with established indicators of aggressive GBM behavior. The positive correlation between age and risk score reinforces age as a contributing prognostic factor. Although MGMT methylation did not differ significantly between risk groups in this cohort, the ability of the gene signature to stratify survival independently of MGMT suggests that it captures molecular features beyond traditional markers. This implies that the synaptic-related signature may serve as a complementary tool rather than a replacement for MGMT, offering additional discrimination power in cases where conventional markers are insufficient. Clinically, this signature has the potential to complement established biomarkers—including MGMT methylation and IDH mutation status—by providing additional molecular stratification to guide individualized treatment planning.

Through this research, a comprehensive prognostic model for GBM was constructed, grounded in transcriptomic changes, and its reliability was substantiated by independent validation across multiple cohorts. Future studies incorporating functional experimentation and prospective clinical cohorts are warranted to elucidate mechanistic roles and support translation into therapeutic strategies.

CONCLUSIONS

This study identified a synaptic pathway-enriched ten-gene prognostic signature (SPRY1, CD58, RCC1, E2F7, BUB1, FAM46A, TYMS, NEDD9, CHST14, and REPS2) that can robustly stratify patients with glioblastoma based on survival risk. The model demonstrated strong predictive accuracy and independence from conventional clinical indicators, suggesting its potential value as a complementary tool for risk assessment and treatment planning. Our results reinforce the contribution of neuron–glioma interactions to GBM progression and highlight synaptic mechanisms as promising therapeutic entry points. While these findings provide a foundation for translational development, further in vitro and in vivo experimental validation, followed by prospective clinical studies, will be essential to confirm the biological relevance of this signature and support its integration into clinical workflows.

Data Availability Statement

The datasets analyzed in this study are publicly available. Transcriptomic and clinical data were obtained from The Cancer Genome Atlas (TCGA), Chinese Glioma Genome Atlas (CGGA), and the Gene Expression Omnibus (GEO) databases. All accession numbers are provided in the Methods section.

ACKNOWLEDGEMENTS

The authors would like to thank Universitas PGRI Adi Buana Surabaya for providing research facilities and administrative support. We also acknowledge the contributors of The Cancer Genome Atlas (TCGA), Chinese Glioma Genome Atlas (CGGA) and the Gene Expression Omnibus (GEO) databases for making their data publicly available.

DECLARATIONS

Grants and Funding Information

This research was supported by the Directorate of Research and Community Service, Directorate General of Research and Development, Ministry of Higher Education, Science, and Technology of the Republic of Indonesia, under Grant Nos. 128/C3/DT.05.00/PL/2025, 037/LL7/DT.05.00/PL/2025, and 040.16/Kontrak/LPPM/VI/2025.

Conflict of Interest

The authors declare that there is no conflict of interest regarding the publication of this article.

Registration Number of Clinical Trial

Not applicable. This study did not involve a clinical trial.

Author Contributions

Conceptualization and methodology: V.A., G.A.; Investigation: V.A., G.A.; Formal analysis: G.A., F.F., S.S.N.; Visualization and writing—original draft: G.A.; Writing—review and editing: V.A., G.A.; Funding acquisition: V.A.; Supervision: V.A., G.A. All authors have read and agreed to the final version of the manuscript.

Use of Artificial Intelligence

During the preparation of this manuscript, the authors used ChatGPT to assist with language editing and to improve the clarity and fluency of the text. The authors subsequently reviewed and edited the content critically and take full responsibility for the accuracy, integrity, and scholarly quality of the work.

REFERENCES

1. Sipos D, Raposa BL, Freihat O, Simon M, Mekis N, Cornacchione P, et al. Glioblastoma: Clinical Presentation, Multidisciplinary Management, and Long-Term Outcomes. Cancers (Basel). 2025; 17(1):146.
2. Pouyan A, Ghorbanlo M, Eslami M, Jahanshahi M, Ziaei E, Salami A, et al. Glioblastoma multiforme: insights into

pathogenesis, key signaling pathways, and therapeutic strategies. Mol Cancer. 2025;24(1):58.
3. Lim-Fat MJ, Wen PY. Glioma progression through synaptic activity. Nat Rev Neurol. 2020;16(1):6-7.
4. Venkataramani V, Yang Y, Schubert MC, Reyhan E, Tetzlaff SK, Wißmann N, et al. Glioblastoma hijacks neuronal mechanisms for brain invasion. Cell. 2022;185(16):2899-917. e31.
5. Dresselhaus EC, Meffert MK. Cellular specificity of NF-κB function in the nervous system. Front Immunol. 2019;10:1043.
6. Zhang GL, Wang CF, Qian C, Ji YX, Wang YZ. Role and mechanism of neural stem cells of the subventricular zone in glioblastoma. World J Stem Cells. 2021;13(7):877-93.
7. Feng J, Yang J. Glioma-neuron interactions: insights from neural plasticity. Front Oncol. 2025;15:1661897.
8. Hua T, Shi H, Zhu M, Chen C, Su Y, Wen S, et al. Glioma-neuronal interactions in tumor progression: Mechanism, therapeutic strategies and perspectives (Review). Int J Oncol. 2022;61(3).
9. Williams JB, Cao Q, Yan Z. Transcriptomic analysis of human brains with Alzheimer's disease reveals the altered expression of synaptic genes linked to cognitive deficits. Brain Commun. 2021;3(3):fcab123.
10. Nguyen DPQ, Pham S, Jallow AW, Ho N-T, Le B, Quang HT, et al. Multiple Transcriptomic Analyses Explore Potential Synaptic Biomarker Rabphilin-3A for Alzheimer's Disease. Sci Rep. 2024;14(1):18717.
11. Bhattacharya A, Stutvoet TS, Perla M, Loipfinger S, Jalving M, Reyners AKL, et al. Transcriptional pattern enriched for synaptic signaling is associated with shorter survival of patients with high-grade serous ovarian cancer. eLife. 2025;13:RP101369.
12. Yoshino Y, Roy B, Kumar N, Shahid Mukhtar M, Dwivedi Y. Molecular pathology associated with altered synaptic transcriptome in the dorsolateral prefrontal cortex of depressed subjects. Transl Psychiatry. 2021;11(1):73.
13. Sun L, Hui AM, Su Q, Vortmeyer A, Kotliarov Y, Pastorino S, et al. Neuronal and glioma-derived stem cell factor induces angiogenesis within the brain. Cancer Cell. 2006;9(4):287-300.
14. Griesinger AM, Birks DK, Donson AM, Amani V, Hoffman LM, Waziri A, et al. Characterization of distinct immunophenotypes across pediatric brain tumor types. J Immunol. 2013;191(9):4880-8.
15. Madhavan S, Zenklusen JC, Kotliarov Y, Sahni H, Fine HA, Buetow K. Rembrandt: helping personalized medicine become a reality through integrative translational research. Mol Cancer Res. 2009;7(2):157-67.
16. Kruthika BS, Jain R, Arivazhagan A, Bharath RD, Yasha TC, Kondaiah P, et al. Transcriptome profiling reveals PDZ binding kinase as a novel biomarker in peritumoral brain zone of glioblastoma. J Neurooncol. 2019;141(2):315-25.
17. Alnaser RI, Abed MN, Alassaf FA, Alsaaty MH. Integrating Artificial Intelligence into Chronic Kidney Disease Care: Enhancing Hemodialysis Scheduling, Comorbidity Management, and Diagnostic Capabilities. Siriraj Med J. 2025;77(7):543-52.
18. Saenmanot N, Ruangchainikom M, Ariyawatkul T, Korwutthikulrangsri E, Saenmanot S, Luksanapruksa P, et al. Survival Analysis of and Prognostic Factors for Metastatic Epidural Spinal Cord Compression Compared between Preoperative Known and Unknown Primary Tumors. Siriraj Med J. 2022;74(10):684-92.
19. Chen EY, Tan CM, Kou Y, Duan Q, Wang Z, Meirelles GV, et al. Enrichr: interactive and collaborative HTML5 gene list enrichment analysis tool. BMC Bioinformatics. 2013;14:128.
20. Kuleshov MV, Jones MR, Rouillard AD, Fernandez NF, Duan Q, Wang Z, et al. Enrichr: a comprehensive gene set enrichment analysis web server 2016 update. Nucleic Acids Res. 2016;44(W1):W90-W97.
21. Xie Z, Bailey A, Kuleshov MV, Clarke DJB, Evangelista JE, Jenkins SL, et al. Gene Set Knowledge Discovery with Enrichr. Curr Protoc. 2021;1(3):e90.
22. Ashburner M, Ball CA, Blake JA, Botstein D, Butler H, Cherry JM, et al. Gene ontology: tool for the unification of biology. Nat Genet. 2000;25(1):25-9.
23. Kanehisa M, Goto S. KEGG: kyoto encyclopedia of genes and genomes. Nucleic acids research. 2000;28(1):27-30.
24. Tian Y, Chen Le, Jiang Y. LASSO-based screening for potential prognostic biomarkers associated with glioblastoma. Front Oncol. 2023;12:1057383.
25. Yu SH, Cai JH, Chen DL, Liao SH, Lin YZ, Chung YT, et al. LASSO and Bioinformatics Analysis in the Identification of Key Genes for Prognostic Genes of Gynecologic Cancer. J Pers Med. 2021;11(11).
26. Kamarudin AN, Cox T, Kolamunnage-Dona R. Time-dependent ROC curve analysis in medical research: current methods and applications. BMC Medical Research Methodology. 2017;17(1):53.
27. Geanphun S, Rerkpichaisuth V, Ruangchira-urai R, Thongcharoen P. Survival of Non-Small Cell Lung Cancer Patients with Unexpected N2 after Complete Resection: Role of Aggressive Invasive Mediastinal Staging Should be Considered. Siriraj Med J. 2022;74(3):161-8.
28. Jia Z, Wu H, Xu J, Sun G. Development and validation of a nomogram to predict overall survival in young non-metastatic rectal cancer patients after curative resection: a population-based analysis. Int J Colorectal Dis. 2022;37(11):2365-74.
29. Tang Z, Li C, Kang B, Gao G, Li C, Zhang Z. GEPIA: a web server for cancer and normal gene expression profiling and interactive analyses. Nucleic Acids Res. 2017;45(W1):W98-W102.
30. Sudhof TC. The synaptic vesicle cycle. Annu Rev Neurosci. 2004;27:509-47.
31. Venkataramani V, Tanev DI, Strahle C, Studier-Fischer A, Fankhauser L, Kessler T, et al. Glutamatergic synaptic input to glioma cells drives brain tumour progression. Nature. 2019;573(7775):532-8.
32. Krishna S, Choudhury A, Keough MB, Seo K, Ni L, Kakaizada S, et al. Glioblastoma remodelling of human neural circuits decreases survival. Nature. 2023;617(7961):599-607.
33. Venkataramani V, Tanev DI, Strahle C, Studier-Fischer A, Fankhauser L, Kessler T, et al. Glutamatergic synaptic input to glioma cells drives brain tumour progression. Nature. 2019;573(7775):532-8.
34. Venkatesh HS, Morishita W, Geraghty AC, Silverbush D, Gillespie SM, Arzt M, et al. Electrical and synaptic integration of glioma into neural circuits. Nature. 2019;573(7775):539-45.
35. Venkataramani V, Tanev DI, Kuner T, Wick W, Winkler F. Synaptic input to brain tumors: clinical implications. Neuro Oncol. 2021;23(1):23-33.
36. Tetzlaff SK, Reyhan E, Layer N, Bengtson CP, Heuer A, Schroers J, et al. Characterizing and targeting glioblastoma neuron-tumor networks with retrograde tracing. Cell. 2025;188(2):390-411. e36.
37. Taylor KR, Barron T, Hui A, Spitzer A, Yalçin B, Ivec AE, et al. Glioma synapses recruit mechanisms of adaptive plasticity. Nature. 2023;623(7986):366-74.
38. Hua T, Shi H, Zhu M, Chen C, Su Y, Wen S, et al. Glioma-neuronal

interactions in tumor progression: Mechanism, therapeutic strategies and perspectives (Review). Int J Oncol. 2022;61(3):104.
39. Sisakht AK, Malekan M, Ghobadinezhad F, Firouzabadi SNM, Jafari A, Mirazimi SMA, et al. Cellular Conversations in Glioblastoma Progression, Diagnosis and Treatment. Cell Mol Neurobiol. 2023;43(2):585-603.
40. Barron T, Yalçın B, Su M, Byun YG, Gavish A, Shamardani K, et al. GABAergic neuron-to-glioma synapses in diffuse midline gliomas. Nature. 2025;639(8056):1060-8.
41. Jovčevska I, Zottel A, Šamec N, Mlakar J, Sorokin M, Nikitin D, et al. High FREM2 Gene and Protein Expression Are Associated with Favorable Prognosis of IDH-WT Glioblastomas. Cancers (Basel). 2019;11(8):1060.
42. Ho P, Melms JC, Rogava M, Frangieh CJ, Poźniak J, Shah SB, et al. The CD58-CD2 axis is co-regulated with PD-L1 via CMTM6 and shapes anti-tumor immunity. Cancer Cell. 2023;41(7):1207-21.e12.
43. Bannoura SF, Aboukameel A, Khan HY, Uddin MH, Jang H, Beal E, et al. Regulator of Chromosome Condensation (RCC1) a novel therapeutic target in pancreatic ductal adenocarcinoma drives tumor progression via the c-Myc-RCC1-Ran axis. bioRxiv [Preprint]. 2023.12.18.572102.
44. Xu K, Li W, Li X, Liu C, Yi C, Tang J, et al. RNA binding motif protein 25 is a negative prognostic biomarker and promotes cell proliferation via alternative splicing in hepatocellular carcinoma. Pathol Res Pract. 2025;269:155941.
45. Xu K, Li W, Li X, Liu C, Yi C, Tang J, et al. RNA binding motif protein 25 is a negative prognostic biomarker and promotes cell proliferation via alternative splicing in hepatocellular carcinoma. Pathol Res Pract. 2025;269:155941.
46. Chen K-q, Lei H-b, Liu X, Wang S-z. The roles of E2F7 in cancer: Current knowledge and future prospects. Heliyon. 2024;10(14).
47. Gugnoni M, Lorenzini E, Faria do Valle I, Remondini D, Castellani G, Torricelli F, et al. Adding pieces to the puzzle of differentiated-to-anaplastic thyroid cancer evolution: the oncogene E2F7. Cell Death Dis. 2023;14(2):99.
48. Hao F, Wang N, Zhang Y, Xu W, Chen Y, Fei X, et al. E2F7 enhances hepatocellular carcinoma growth by preserving the SP1/SOX4/Anillin axis via repressing miRNA-383-5p transcription. Mol Carcinog. 2022;61(11):975-88.
49. Kim T, Gartner A. Bub1 kinase in the regulation of mitosis. Anim Cells Syst (Seoul). 2021;25(1):1-10.
50. Huang W, Chen Z, Tang Y, Li J, Fan L. A Pan-Cancer Analysis of the Immunological and Prognostic Role of BUB1 Mitotic Checkpoint Serine/Threonine Kinase B (BUB1B) in Human Tumors. Clin Lab. 2024;70(1).
51. Pokaew N, Prajumwongs P, Vaeteewoottacharn K, Wongkham S, Pairojkul C, Sawanyawisuth K. Overexpression of BubR1 Mitotic Checkpoint Protein Predicts Short Survival and Influences the Progression of Cholangiocarcinoma. Biomedicines. 2024;12(7):1611.
52. Liang S, Yueyang L, Jianhui H, Tian G, Lanying L, and He S. Family with sequence similarity 46 member a confers chemo-resistance to ovarian carcinoma via TGF-β/Smad2 signaling. Bioengineered. 2022;13(4):10629-39.
53. Guijarro MV, Nawab A, Dib P, Burkett S, Luo X, Feely M, et al. TYMS promotes genomic instability and tumor progression in Ink4a/Arf null background. Oncogene. 2023;42(23):1926-39.
54. Geng Y, Xie L, Wang Y, Wang Y. Unveiling the oncogenic significance of thymidylate synthase in human cancers. Am J Transl Res. 2024;16(10):5228-47.
55. Zhang F, Ye J, Guo W, Zhang F, Wang L, Han A. TYMS-TM4SF4 axis promotes the progression of colorectal cancer by EMT and upregulating stem cell marker. Am J Cancer Res. 2022;12(3):1009-26.
56. Yu HG, Bijian K, da Silva SD, Su J, Morand G, Spatz A, et al. NEDD9 links anaplastic thyroid cancer stemness to chromosomal instability through integrated centrosome asymmetry and DNA sensing regulation. Oncogene. 2022;41(21):2984-99.
57. Purazo ML, Ice RJ, Shimpi R, Hoenerhoff M, Pugacheva EN. NEDD9 Overexpression Causes Hyperproliferation of Luminal Cells and Cooperates with HER2 Oncogene in Tumor Initiation: A Novel Prognostic Marker in Breast Cancer. Cancers. 2023;15(4):1119.
58. Han D, Owiredu JN, Healy BM, Li M, Labaf M, Steinfeld JS, et al. Susceptibility-Associated Genetic Variation in NEDD9 Contributes to Prostate Cancer Initiation and Progression. Cancer Res. 2021;81(14):3766-76.
59. Zhan J, Zhou L, Zhang H, Zhou J, He Y, Hu T, et al. A comprehensive analysis of the expression, immune infiltration, prognosis and partial experimental validation of CHST family genes in gastric cancer. Transl Oncol. 2024;40:101843.
60. Zhang H, Duan CJ, Zhang H, Cheng YD, Zhang CF. Expression and clinical significance of REPS2 in human esophageal squamous cell carcinoma. Asian Pac J Cancer Prev. 2013;14(5):2851-7.
61. He Z, Wang C, Xue H, Zhao R, Li G. Identification of a Metabolism-Related Risk Signature Associated With Clinical Prognosis in Glioblastoma Using Integrated Bioinformatic Analysis. Front Oncol. 2020;10:1631.
62. Liu X, Liu X. A novel immune-related gene prognostic signature combining immune cell infiltration and immune checkpoint for glioblastoma patients. Transl Cancer Res. 2024;13(11):6136-53.
63. Su Y, Yang DS, Li Yq, Qin J, Liu L. Early-onset locally advanced rectal cancer characteristics, a practical nomogram and risk stratification system: a population-based study. Front Oncol. 2023;13:1190327.
64. Yang D, Zhu M, Xiong X, Su Y, Zhao F, Hu Y, et al. Clinical features and prognostic factors in patients with microvascular infiltration of hepatocellular carcinoma: Development and validation of a nomogram and risk stratification based on the SEER database. Front Oncol. 2022;12:987603.
65. Doolan P, Clynes M, Kennedy S, Mehta JP, Germano S, Ehrhardt C, et al. TMEM25, REPS2 and Meis 1: Favourable Prognostic and Predictive Biomarkers for Breast Cancer. Tumor Biology. 2009;30(4):200-9.